ELSEVIER

NeuroImage

www.elsevier.com/locate/ynimg
NeuroImage 22 (2004) 1790–1801

Deformable registration of cortical structures via hybrid volumetric and surface warping

Tianming Liu,* Dinggang Shen, and Christos Davatzikos

Section of Biomedical Image Analysis, Department of Radiology, University of Pennsylvania, Philadelphia, PA 19104, USA

Received 3 February 2004; revised 5 April 2004; accepted 21 April 2004

Registration of cortical structures across individuals is a very important step for quantitative analysis of the human brain cortex. This paper presents a method for deformable registration of cortical structures across individuals, using hybrid volumetric and surface warping. In the first step, a feature-based volumetric registration algorithm is used to warp a model cortical surface to the individual's space. This step greatly reduces the variation between the model and individual, thus providing a good initialization for the next step of surface warping. In the second step, a surface registration method, based on matching geometric attributes, warps the model surface to the individual. Point correspondences are also established at this step. The attribute vector, as the morphological signature of surface, was designed to be as distinctive as possible, so that each vertex on the model surface can find its correspondence on the individual surface. Experimental results on both synthesized and real brain data demonstrate the performance of the proposed method in the registration of cortical structures across individuals.

Keywords: Deformable registration; Cortical structures; Hybrid warping

Introduction

Registration of cortical structures across individuals is a very important step for quantitative analysis of the human brain cortex. Having registered cortical structures, one can perform group or individual analysis of these structures to assess normal group differences in terms of age, gender, genetic background, handedness, etc. (Ashburner et al., 2003; Davatzikos and Bryan, 2002; Mangin et al., 2003; Thompson et al., 2001b). Also, we can define disease-specific signatures and detect individual cortical atrophy, based on certain computational anatomy methods (May et al., 1999; Thompson et al., 2001a; Toga and Thompson, 2003). Moreover, registration of cortical structures has many other applications such as automatic cortical structure labeling and visualization (Le Goualher et al., 1999), functional brain mapping (Toga and Mazziotta, 2000), and neurosurgical planning (Kikinis et al., 1991).

In recent years, registration of cortical surfaces has received increasing interest as a research goal. An early approach by Talairach and Tournoux (1988) normalized the individual brains into a standard space and has been extensively employed due to its ease of use. However, the accuracy of this method is limited, e.g., the intersubject variabilities in the locations of cortical anatomical landmarks after Talairach alignment are at the order of centimeters (Thompson and Toga, 1996; Van Essen et al., 1998). Hence, there have been several methods proposed to improve the accuracy of cortical structure registration, which fall into two categories. The first category of methods registers the cortical surfaces in the standard space into which all the cortical surfaces are mapped (Angenent et al., 1999; Davatzikos and Bryan, 1996; Fischl et al., 1998, 1999; Tao et al., 2002; Thompson and Toga, 1996; Thompson et al., 2002; Tosun et al., 2003). The major advantages of these methods include the easy visualization of the highly convoluted cortical surfaces and the maintenance of topology of the cortical surfaces. However, there exists unavoidable distortion in the mapping of cortical surfaces into the standard space. The second category of methods uses landmarks, automatically or manually labeled, to guide the registration of cortical surfaces (Chui, 2001; Feldmar and Ayache, 1994; Liu et al., 2003; Thompson et al., 2001b; Van Essen et al., 1998; Wang et al., 2003). The accuracy of these methods depends on how well the landmarks are labeled, and as well as how accurate the warping method is performed.

In this paper, we present a hybrid warping method for the registration of cortical surfaces that combines the advantages of volumetric and surface warping methods. In particular, throughout the paper, we will assume that a model cortical surface that belongs to a template brain, is warped to the subject space using a feature-based volumetric registration algorithm (Shen and Davatzikos, 2002). This step greatly removes the variability between the cortical surfaces of the model and the individual, and places the model's cortical surface close to the individual's cortical surface, thereby providing a good initialization for the subsequent surface registration. In the surface warping step, an attribute-based surface registration method further refines the cortical registration results obtained from the volumetric warping step. An attribute vector is defined for each vertex in the cortical surface, and used to characterize both local and global geometric structures around that vertex. The attribute vector is designed to

* Corresponding author. Department of Radiology, University of Pennsylvania, Suite 380, 3600 Market Street, Philadelphia, PA 19104.
E-mail address: tliu@rad.upenn.edu (T. Liu).
Available online on ScienceDirect (www.sciencedirect.com.)

1053-8119/$ - see front matter © 2004 Elsevier Inc. All rights reserved.
doi:10.1016/j.neuroimage.2004.04.020

be as distinctive as possible to distinguish the different parts of the cortical surface. In effect, the attribute vector of a vertex on the cortical surface serves as its morphological signature that subsequently guides the surface warping.

Method

Overview

Our cortical surface registration method can be formulated as a procedure of warping the model surface to the subject surface, h: $S^{\text{Mdl}} \rightarrow S^{\text{Sub}}$, where S^{Mdl} and S^{Sub} are model and subject surfaces, respectively, and h is the desired transformation. The warping h can be decomposed into two steps: a volumetric warping step h_1 and a surface warping step h_2, i.e., $h = h_2 \circ h_1$. The first transformation h_1 is obtained by a volumetric warping method (Shen and Davatzikos, 2002) called HAMMER, which results in a volumetrically warped model surface $S^{\text{W\_Mdl}}$, i.e., $S^{\text{W\_Mdl}} = h_1(S^{\text{W\_Mdl}})$. The second transformation h_2 is determined by an attribute-based surface warping method, which results in a finally warped model surface S^{Final}, i.e., $S^{\text{Final}} = h_2(S^{\text{W\_Mdl}})$. All procedures in our hybrid warping method are summarized in Fig. 1.

As we are warping one cortical surface to another, the reconstruction of the cortical surface from magnetic resonance (MR) images is a prerequisite for the surface-based registration method. Therefore, we firstly introduce our method for reconstructing topologically correct cortical surfaces.

Reconstruction of a topologically correct cortical surface

Reconstructing topologically correct and geometrically accurate cortical surfaces from MRI images is a challenging problem (Dale et al., 1999; Davatzikos and Bryan, 1996; Han et al., 2003; Kriegeskorte and Goebel, 2001; MacDonald et al., 2000; Shattuck and Leahy, 2001; Xu et al., 1999; Zeng et al., 1998). Incorrect reconstruction of cortical surfaces can lead to incorrect interpretations of local structural relationships, thereby affecting the performance of the later stage of attribute-based surface registration, because the calculation of attribute vectors is highly dependent on the geometry of the surface.

There have been several methods that attempt to automatically produce topologically correct cortical segmentations. The homotopically deformable region model proposed in Mangin et al. (1995) is one of the earliest works. It starts with an initial region with the required topology, and then grows the region by adding simple points, whose addition or removal will not change the topology (Bertrand, 1994; Kong and Rosenfeld, 1989; Saha and Chaudhuri, 1994). More recently, deformable surfaces have been used to generate topologically correct cortical surface representations (Davatzikos and Bryan, 1996; MacDonald et al., 2000; Xu et al., 1999). The advantage of parametric deformable surface model is that the topology of the final surface is identical to that of the initial one provided that the deformation process is topology preserving. Alternatively, geometric deformable surface models have been used to generate cortical surfaces (Han et al., 2003; Zeng et al., 1998). In particular, a topology-preserving geometric model was introduced to reconstruct inner, outer, or central cortical surfaces in Han et al. (2003).

Recently, Shattuck and Leahy (2001) described an algorithm for topology correction in a digital volume image. Their method builds graphs that encode the connectivity of both foreground and background voxels, respectively. Then, the problem of handle removal is formulated as removing the cycles in the connectivity graphs, because the authors assumed that there is no cycle in the connectivity graphs if the expected surface is homeomorphic to a sphere. This assumption was later proved to be correct by Abrams et al. (2002).

We use a method very similar to that in Shattuck and Leahy (2001) to perform topology correction. Firstly, the scanned T1 MR brain image is skull-stripped. Then, the brain tissues are classified into White Matter (WM), Gray Matter (GM), and CSF (Goldszal et al., 1998). Finally, for the WM volume image, we use the same method as Shattuck and Leahy (2001) to construct both foreground and background connectivity graphs, whose edge weight represents the strength of connection between nodes in

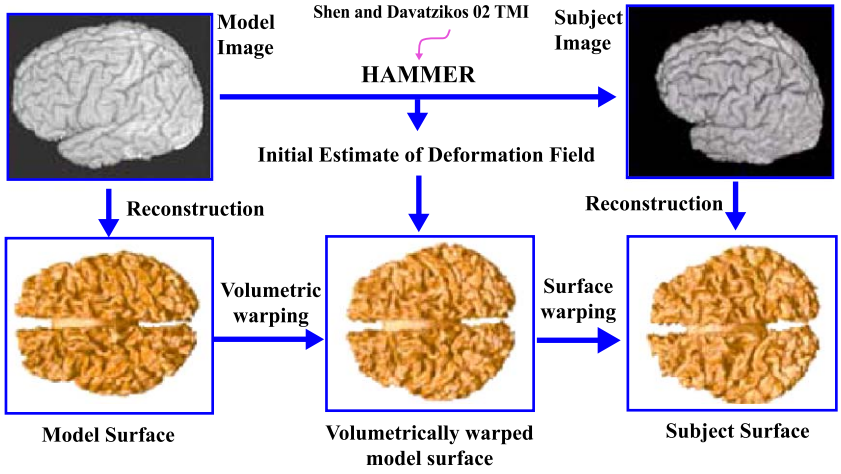

Fig. 1. The flowchart of the hybrid warping method. Firstly, HAMMER registers the model image and subject image, and produces an initial estimate of the deformation field. Then, the cortical surfaces are reconstructed from both volume images of model and subject; and the model cortical surface is warped into subject space using the deformation field provided by the HAMMER algorithm. Finally, a surface warping method is used to refine the results of volumetric warping. The model and subject brain images are arbitrarily selected from the BLSA data set (Goldszal et al., 1998).

adjacent slices. Notably, the constructed connectivity graphs can also be called Reeb graphs (Wood, 2003), and the cycles in the Reeb graph are actually indicators of handles. Therefore, removing handles is equal to removing cycles in the graph. We use the Prim-Dijkstra's algorithm (Cormen et al., 1990) to produce maximal spanning trees from the connectivity graphs, and remove the weakest connections in the connectivity graphs. During the handle removal, we also iteratively perform the in-place correction along each axis (x, y, and z). Importantly, only a limited number of voxels are allowed to be corrected in each correction operation, and the number of voxels allowed to correct is designed to decrease with the increase of iterations. This particular correction strategy improves the performance of our topology correction algorithm. Fig. 2 shows an example of the topology correction for a WM volume, where a handle was removed by filling the background.

After topology correction, we use the marching cubes algorithm (Lorensen and Cline, 1987) to reconstruct an isosurface of the WM volume. Because the traditional marching cubes algorithm usually produces holes in the isosurface due to the ambiguities in marching cubes, we instead use an improved marching cubes method proposed in Nielson and Hamann (1991), which employs an asymptotic decider to resolve the problem of ambiguities in marching cubes. By using this surface reconstruction method, we can obtain both the model surface S^{Mdl} and the individual surface S^{Sub}, which will be used in hybrid warping.

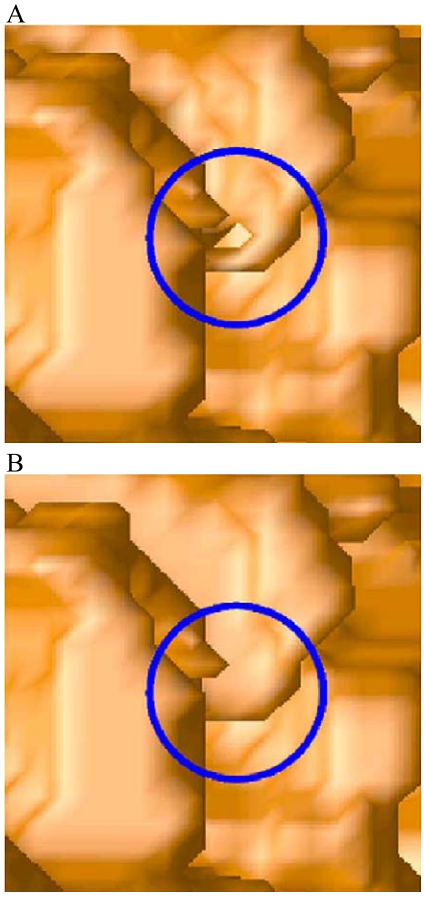

Fig. 2. An example of the topology correction on WM volume. (A) Before correction. (B) After correction. The handle is removed by filling the background in the WM volume.

Volumetric warping

Having the model cortical surface, we firstly warp it into the subject space using the deformation field produced by a volumetric warping method. Many registration methods can be used for volumetric registration of brain images (Ashburner and Friston, 1997; Bajcsy et al., 1983; Collins et al., 1994; Davatzikos, 1997; Evans et al., 1991; Gee et al., 1994; Joshi et al., 1996; Rueckert et al., 1999; Thirion et al., 1992; Thompson and Toga, 1996; Wells et al., 1996; Woods et al., 1998), having varying degrees of flexibility and optimality criterion. We use a registration method called HAMMER (Shen and Davatzikos, 2002, 2003), because this method achieves relatively high accuracy in matching cortical gyrations. The performance of the HAMMER algorithm is highly related to the use of two novel techniques as listed below.

Firstly, to maximally reduce the ambiguity in image matching, an attribute vector is defined for each voxel and used to characterize the geometric structure around that voxel. The attribute vector is designed to be as distinctive as possible of its respective voxel, to facilitate automated image matching. The attribute vector includes image intensity, edge type information, and several geometric moment invariants (GMIs), which are calculated at different scales to reflect the anatomy in the neighborhood of the voxel.

Secondly, to minimize the chances of avoiding local minima in image matching, a sequence of hierarchical approximations of the energy function is performed by hierarchically selecting the active voxels to drive the volume deformation. Specifically, a few voxels are selected to drive the deformation procedure initially. These active voxels have quite distinctive attribute vectors, and typically lie on roots of sulci or crowns of gyri, as well as on other distinctive structures such as the anterior horn of the ventricles or on parts of the caudate nucleus. As the algorithm progresses, more and more active voxels are added, increasing the dimensionality of the energy function and thus rendering the matching function less and less smooth. This hierarchical approximation of the energy function greatly reduces ambiguities in finding correspondences, and thus reduces the chances of local minima.

By using the transformation h_1 produced by the HAMMER-based volumetric warping method, the model surface S^{Mdl} can be warped to the subject space. Notably, we impose the constraint of topology preservation during the volumetric warping of the model cortical surface, which will be further detailed, together with the topology preservation of surface warping, in the last subsection. After the volumetric warping, the model and subject cortical surfaces become similar, thereby providing a good initialization for the next step of surface warping, which will further refine the warping of $S^{\mathrm{W\_Mdl}}$ to the subject surface S^{Sub}.

Surface warping

Attribute vector

An attribute vector, which we refer to as clamp histogram, is defined for each vertex of the cortical surface, and used to capture both local and global geometric features of the surface around the vertex under consideration. The attribute vector is designed to be

as distinctive as possible, so that each vertex in the model surface can easily find its corresponding one in the individual surface. Actually, in the surface matching literature, various attributes have been used for surface matching, such as COSMOS (Dorai and Jain, 1997), spin-image matching (Johnson and Hebert, 1999), harmonic image matching (Zhang and Hebert, 1998), fingerprint feature matching (Sun and Abidi, 2001), or surface signature matching (Yamany and Farag, 2002).

The definition of the clamp histogram is intuitive, and it is based on the observation that the normal direction changes on the cortical surface embody rich geometric information, e.g., more rapid changes in the roots of sulci or crowns of gyri than those in other flat regions. Actually, the normal direction changes around a surface vertex can be used to define the morphological signature for that vertex, e.g., the normal direction changes is linked to curvatures that were used widely in surface representation and registration.

The clamp histogram is the accumulation of angles between the normal direction of a vertex under consideration, denoted as v, and the normal directions of its neighboring vertices $\{v_j \in P(v,r)\}$, where $P(v,r)$ is a surface patch centered on the vertex v and with a geodesic distance of r. Essentially, the clamp histogram can be calculated within a neighborhood of arbitrarily large geodesic distance, i.e., within the whole surface. By this we do not mean that the entire surface is used in determining the attribute vector, but rather that relatively more distant relationships between vertices are captured. In this paper, we use $r = 20$ mm as it brings acceptable computation burden while providing good performance. As demonstrated in Fig. 3a, the angle between the normal direction of vertex v and the normal direction of its neighboring vertex v_j can be calculated by

$$\alpha_j = \cos^{-1}(n(v)n(v_j)) \tag{1}$$

where $n(\cdot)$ denotes the normal direction of a vertex, and angle α_j is in the range of $[0,\pi]$. Then, for each neighbor of vertex v within a geodesic distance, we perform the same angle calculation as indicated in Figs. 3b and c. Notably, the use of geodesic distance is preferred here to Euclidean distance because this is very important to calculate consistent attribute vectors across individuals. To calculate the histogram of the angles, the entire angle range $[0,\pi]$ is divided into N equal segments, and each segment counts the accumulation of angles in its domain. In this study, we use $N = 18$. Let $\{h(v,k), k \in [1,N]\}$ denote the histogram of angles for the vertex v; then, the vector $A(v) = [h(v,1),\ldots,h(v,N)]^T$ is used as an attribute vector for vertex v, to represent geometric information of the surface patch around vertex v. To make clamp histogram comparable for surfaces with different resolutions, the clamp histogram is normalized as

$$A(v) = \left[\frac{H(v,1)}{N},\cdots,\frac{H(v,N)}{N}\right]^T$$

where

$$N = \sum_{i=1}^{N} H(v,i)$$

To demonstrate the distinctiveness of the clamp histogram, Fig. 4 shows the color-coded similarity between the clamp histogram of vertex A and the clamp histograms of its neighbors. The clamp histogram attribute vector can distinguish one vertex from another, for two reasons. First, because the directions of normal vectors rapidly vary along the cortical surface, the neighboring vertices possess quite different attribute vectors, and this can easily be distinguished using clamp histogram, as long as a surface patch of sufficient size is used. Second, the cortical surface is highly irregular and highly convoluted, which gives the distant vertices very different attribute vectors. In addition to distinctiveness, another important property of clamp histogram is that it is invariant to rigid transformation. Therefore, the clamp histogram attribute vector can be used to directly detect the correspondences of vertices during the registration of cortical surfaces. To reduce computation time, the 1-D clamp histogram, rather than the 2-D maps (Johnson and Hebert, 1999; Yamany and Farag, 2002), is used here.

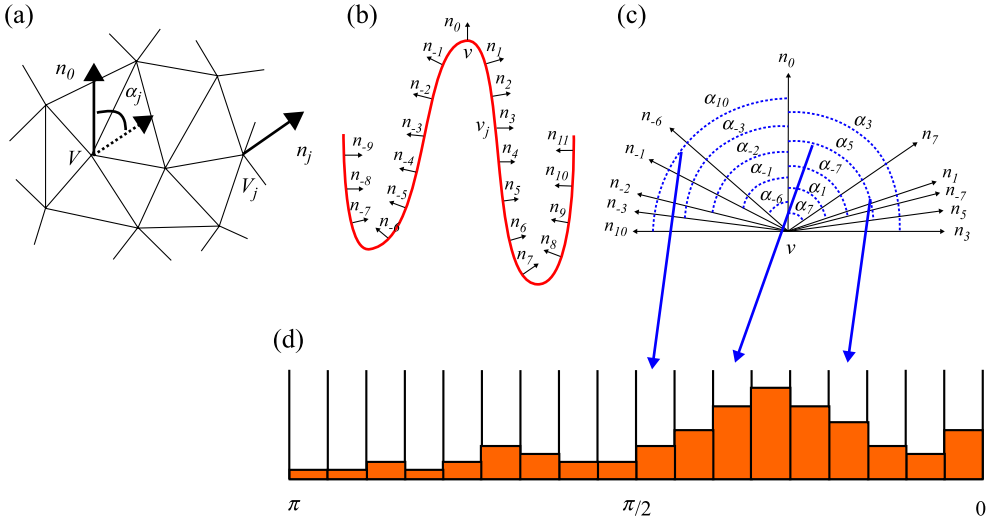

Fig. 3. Schematic illustration of the clamp histogram. (a) The angle between the normal direction of vertex v and the normal direction of its neighbor v_j. (b) The normal directions of the neighbors of v within a geodesic distance, denoted as v_j. (c) The angles between the normal direction of v and the normal directions of its neighbors, denoted as α_j. (d) A histogram of the angle values.

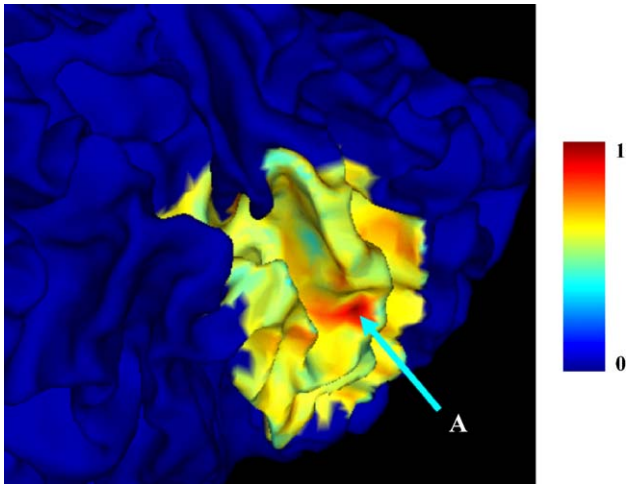

Fig. 4. Demonstration of attribute vectors' ability to distinguish vertices in the cortical surface. The degrees of similarity between the attribute vector of vertex A and the attribute vectors of vertices in its neighborhood are color-coded by a color bar on the right. Red represents high similarity, while blue denotes low similarity.

Objective function in surface warping

The goal of surface warping is to further deform the volumetrically warped model surface $S^{\text{W\_Mmdl}}$ to the individual surface S^{Sub}, using an attribute-based surface matching method. For each model vertex v in the volume-warped model surface $S^{\text{W\_Mmdl}}$, we seek its correspondence in the subject surface S^{Sub}. If the correspondence is successfully determined, the surface patch $P(v,r)$ around the model vertex v will be deformed to the subject surface by a local transformation T_v. Therefore, the transformation h_2 in the second warping step is decomposed into many local transformations $\{T_v = h_2(v)\}$. Mathematically, the surface warping procedure can be formulated as a procedure of minimizing the energy function (McInerney and Terzopoulos, 1996; Terzopoulos and Fleischer, 1988). The energy function is defined as follows.

$$E(h_2 = \{T_v\}) = \sum_{v \in S^{W_{\text{Mdl}}}} y_v \left(w_{\text{Ext}} E_v^{\text{Ext}}(T_v) + w_{\text{Int}} E_v^{\text{Int}}(T_v) \right) \tag{2}$$

where $E_v^{\text{Ext}}(T_v)$ and $E_v^{\text{Int}}(T_v)$ are external and internal energy terms, defined for the model vertex v. W_{Ext} and W_{Int} are weighting parameters for external and internal energy terms, respectively. y_v is the level of our confidence in finding the correct correspondence for vertex v, which will be described in the next subsection of adaptive deformation. Here, different model vertices are weighted differently according to their degrees of confidence.

The external energy term $E_v^{\text{Ext}}(T_v)$ measures the similarity of the surface patches in the model and the subject, respectively. It requires that the clamp histogram of the neighboring vertex v_j in the surface patch $P(v,r)$ be similar to that of its counterpart in the subject surface, and also the normal direction on vertex v_j be close to that on its counterpart. The mathematical definition is given as:

$$E_v^{\text{Ext}}(T_v) = \sum_{v_j \in P(v,r)} \left(w_1 \left\| A(v_j) - A(m(T_v(v_j))) \right\| + w_2 \left\| n(v_j) - n(m(T_v(v_j))) \right\| \right) \tag{3}$$

where $m(\cdot)$ denotes the projection of a point to the closest vertex in the subject surface, because the transformed vertex $T_v(v_j)$ is not necessary on the subject vertex. $n(v_j)$ denotes the normal direction of v_j. w_1 and w_2 are weighting parameters. The operation $\|\cdot\|$ calculates the magnitude of vector. In above external energy definition, both local and global geometric information of the vertex under consideration is taken into account. The clamp histogram does not only contain local information, as curvature does, but it also encodes more distant relationships. In addition to being a distinctive attribute vector, the clamp histogram is also expected to be robust to various forms of noise. This is the key difference between the proposed method and other methods based on curvature matching (Davatzikos, 1997; Fischl et al., 1999b).

The internal energy term $E_v^{\text{Int}}(T_v)$ is designed to preserve the shape of the model surface during the deformation. As proposed in Shen et al. (2001), a geometric attribute vector can be defined for each vertex v, which is actually several volumes of tetrahedrons, formed by the vertex v and its three neighboring vertices in the different neighborhood layers. For example, $F(v)$ is a geometric attribute vector of the vertex v in the volume-warped model surface $S^{\text{W\_Mdl}}$, and $F(T_v(v))$ is the geometric attribute vector of the vertex $T_v(v)$, deformed from v by a local transformation T_v. Then, the internal energy function is defined as:

$$E_v^{\text{Int}}(T_v) = \sum_{v_j \in P(v,r)} \left\| F(v_j) - F(T_v(v_j)) \right\| / N_P(v,r) \tag{4}$$

where $N_P(v,r)$ is the number of vertices in $P(v,r)$. This internal energy favors deformations that tend to maintain relative vertex positions, except for affine transformations. We use a greedy deformation algorithm to minimize energy function in Eq. (2). We deform the surface vertices within a small patch around each model vertex together, rather than deforming only one vertex. This increases the chances of avoiding local minima.

Adaptive deformation

It is well known that there is tremendous morphological variation in the human cortex, which can introduce many local minima during the minimization of the energy function in Eq. (2). To address this problem, we use an adaptive deformation strategy to reduce the chances of being trapped in local minima. The basic

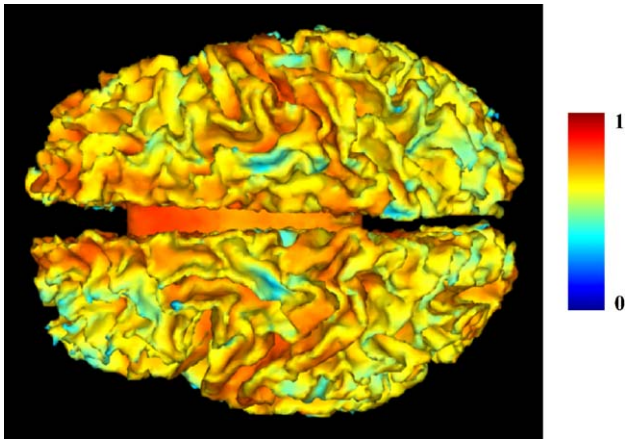

Fig. 5. Color coding of the averaged attributed vector similarity between the model and 60 individuals, which is used as a confidence map to guide the adaptive deformation of cortical structures.

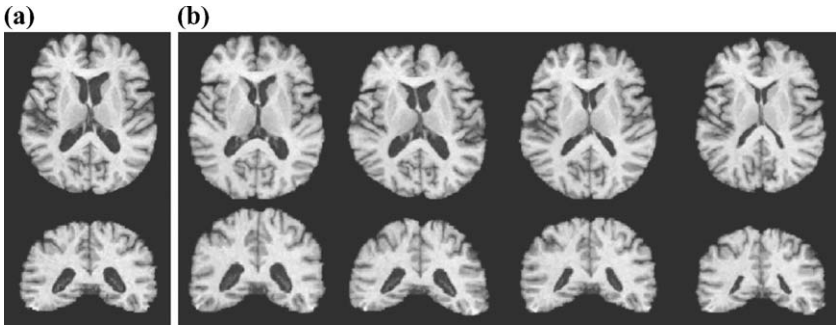

Fig. 6. Synthesized brain images. (a) Model image. (b) Synthesized images obtained by expert definition of a number of sulci and use of them as constraints in an elastic transformation.

idea is that some cortical structures are relatively more consistent across individuals, therefore engendering more confidence that we will find correspondences for these structures. For this reason, our approach deforms these structures first, while other structures with low confidences follow the deformation of the high-confidence neighboring structures. Our adaptive deformation strategy is similar to that proposed in Shen et al. (2001), although the schemes in defining confidences are quite different, as described next.

The confidence in model structures is defined as the similarity between the attribute vector of the model structure and that of the matched subject structure. Fig. 5 shows the averaged clamp histogram attribute vector similarity between the model and 60 individuals. In areas such as precentral gyrus, superior frontal gyrus, Sylvian fissure, and corpus callosum, the similarity is higher than in other areas. Therefore, these structures are relatively more consistent across individuals. Thus, it is natural that we have higher confidence in these structures, and thus the deformation of these structures should initially dominate the deformation of the whole surface. On the other hand, in areas such as medial frontal gyrus, the similarity is relatively lower. Therefore, these areas are less consistent across individuals; hence we have lower confidence in these structures during the deformation process. Our adaptive deformation scheme based on the confidence map is akin to the one proposed in Crum et al. (2003), which emphasizes the importance of understanding and measuring the degree, regional variation, and confidence in the correspondences established by registration. Notably, the confidence map is not available initially; thereby we obtain it by employing the hybrid warping method without using the adaptive deformation strategy. After the confidence map has been generated, we can use it as priori knowledge for adaptive surface warping.

Topology preservation

Topology preservation (Johnson and Christensen, 2002; Musse et al., 2001) is a constraint that ensures that connected structures remain connected, and that the neighborhood relationship between structures is maintained. It also prevents the disappearance or appearance of structures. However, preserving topology during registration is a challenging task. Preserving topology is particularly challenging for the registration of brain images or cortical structures across individuals, because the human cortex is highly convoluted and highly irregular, as well as highly variable.

Topology-preserving warping has already been considered by many investigators. Christensen et al. (1996) introduced viscous fluid material deformation models by using the partial derivative equations. This model allows large displacement estimation compared to elastic Lagrangian approaches, while ensuring topology preservation. Ashburner et al. (1999) preserved the topology by constraining the determinants of the Jacobians of the transformation to be positive for both forward and backward warpings. In Musse et al. (2001), a novel constrained hierarchical parametric approach is presented to ensure that the mapping is completed globally one-to-one and thus preserves topology in the finally deformed image. In Karacali and Davatzikos (2003), a general optimality-based formalism to impose topology-preserving regularity on a given irregular deformation field was presented.

In our hybrid warping algorithm, we want to make sure that both volumetric and surface warping steps preserve topology, so that the finally warped model surface also preserves its topology. As the parametric deformable model is used in the hybrid warping algorithm, we need the implementation of an algorithm

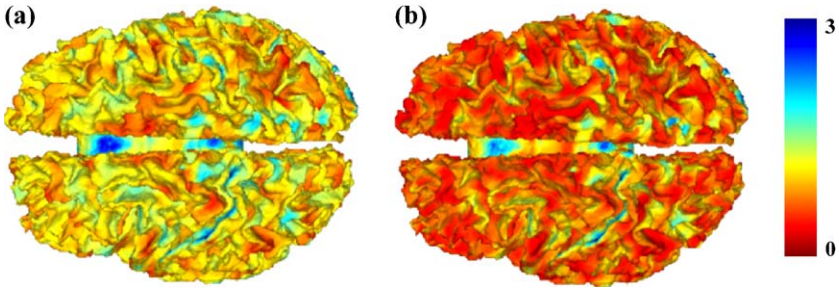

Fig. 7. Registration errors on a synthesized image. Registration errors in millimeters are color-coded by a color bar on the right. (a) Registration errors resulting from a volumetric warping step. (b) Registration errors resulting from a hybrid registration method.

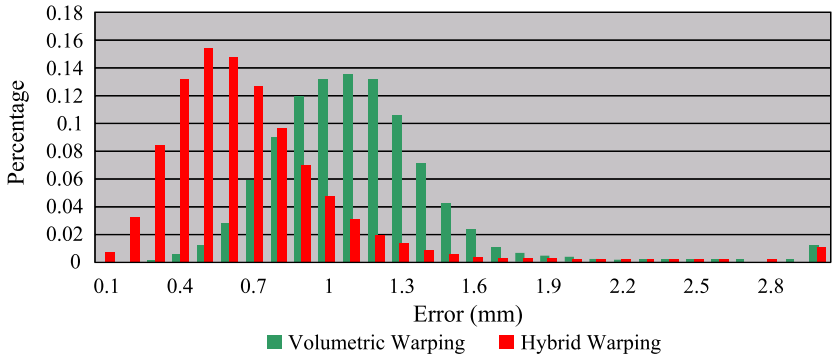

Fig. 8. Histogram of registration errors as given in Fig. 7. The blue bars and red bars denote the results of the volumetric warping step and the results of the hybrid warping methods, respectively.

to explicitly prevent self-intersections. In MacDonald et al. (2000), the explicit prevention of self-intersecting surface geometries is provided by defining both the self-proximity term and the intersurface proximity term in the energy function. The self-proximity term was used to explicitly prevent nonsimple topologies by assigning a prohibitively high cost to self-intersecting topologies. On the other side, the intersurface proximity term was formulated in a similar fashion, and was used to prevent two surfaces from coming within a certain distance of each other. Actually, the most straightforward implementation of explicit prevention of surface self-intersection is to check self-intersection in each deformation step. However, such an algorithm would have very high computational complexity. For example, a single iteration using such an exhaustive approach would require hours on a reasonably sized tessellation, which makes the procedure practically impossible at the current time. Instead, we dramatically reduce the number of triangles to be tested using a method similar to that in Dale et al. (1999). In this method, each point in its subvolume contains a list of faces that intersect it. As the surface is deformed, each vertex is tentatively moved by a short distance. Next, the faces attached to the vertex are examined for self-intersection. This checking is accomplished by using the highly optimized triangle–triangle intersection algorithm described by Möller (1997). If self-intersection is detected, the movement delta is cropped to a point where the self-intersection no longer takes place. We have used the above method to prevent self-intersection for both volumetric and surface warpings, which ensures the finally warped model surface to be not self-intersected.

Results

In this section, we describe a series of experiments to evaluate the hybrid warping method. Both synthesized brain images and real brain images are used to demonstrate the performance of the proposed hybrid method in registering cortical surfaces.

Experiment 1

In this experiment, we use synthesized brain images to quantitatively evaluate the registration accuracy. To get synthesized images, we manually painted major sulci on the model and individuals, and used them as constraints to warp the model into individuals using the STAR algorithm (Davatzikos, 1997). Additional details of the procedures are referred to in Shen and Davatzikos (2002). Fig. 6 shows one slice of each of the synthesized brain images. For the synthesized images, we know the exact correspondences of vertices in their cortical surfaces. In this way, we can directly compare the registration errors that occur when using only the volumetric warping step, with those that occur when using the hybrid volumetric and surface warping method. As visually displayed in Fig. 7, the registration result was improved by using a surface-based warping step. In Fig. 7, the red-shaded area denotes a small registration error, while the blue-shaded area denotes a large registration error. We also use the histogram of registration errors to observe the effect of surface-based warping. As shown in Fig. 8, the overall registration errors have been reduced through use of the surface warping,

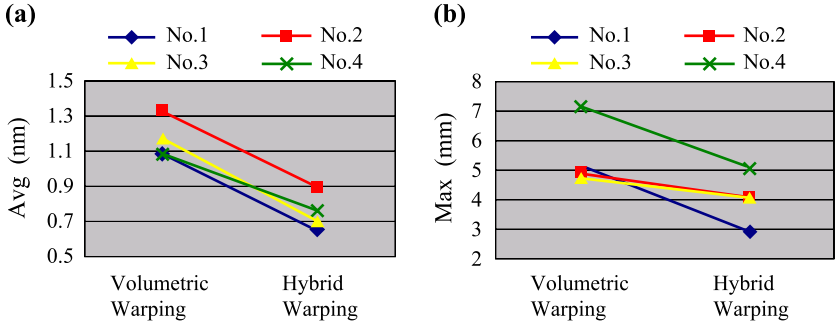

Fig. 9. Average and maximal registration errors on four synthesized images. (a) Average registration errors. (b) Maximal registration errors. It can be observed that the surface warping step improved the registration results obtained from the volumetric warping step.

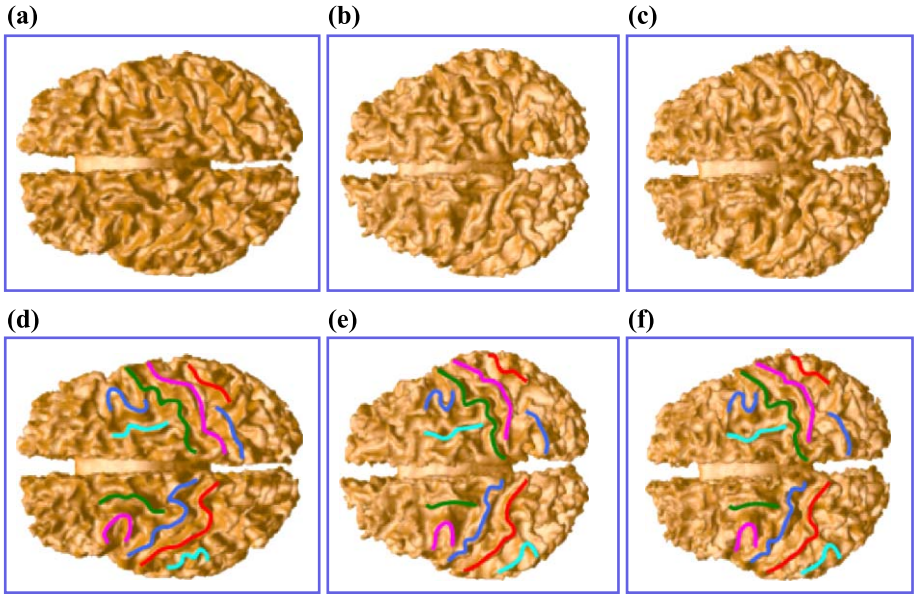

Fig. 10. Visual evaluation of the hybrid warping. The colored curves denote some of the manually painted major gyri of the inner cortical surface. (a) Model surface. (b) Subject surface. (c) Warped model surface using the hybrid method. (d) Model surface, and painted gyri. (e) Subject surface, and painted gyri. (f) Warped model surface using the hybrid method, and colored gyri copied from (e).

reflected as a shifting of the histogram in the direction of smaller errors. The average registration error for this selected synthesized brain is reduced by 30%. Fig. 9 shows additional comparisons over four synthesized brain images, with Fig. 9a showing the comparison on average registration errors, and Fig. 9b showing the comparison on maximal registration errors. By using the surface warping step, the average registration error is reduced by 0.2 mm, and the average maximal error is reduced by 1.4 mm. Notably, for those four synthesized brain images, the hybrid volumetric and surface warping method produced an average

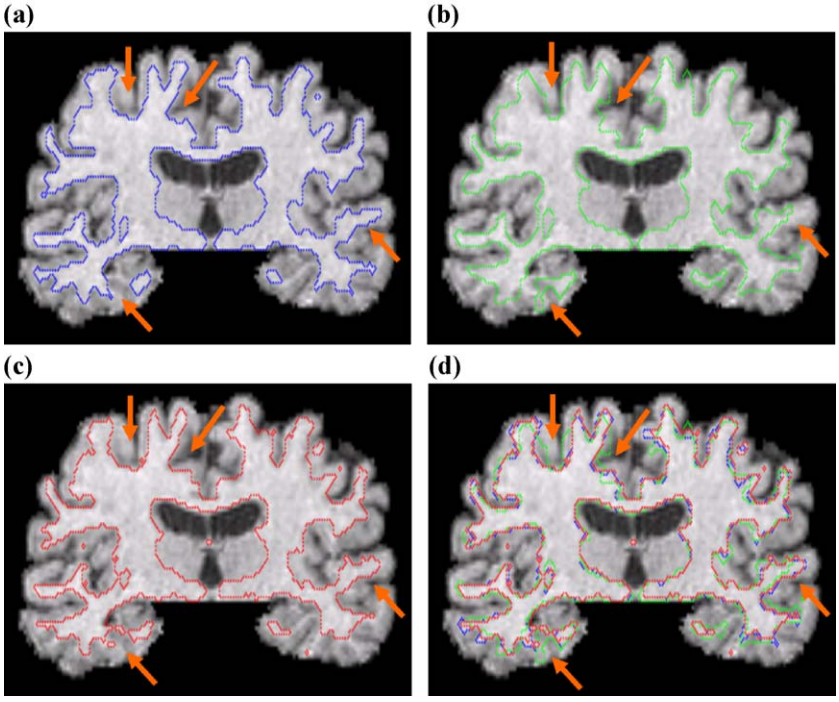

Fig. 11. Visual evaluation of the hybrid warping method in registering cortical surfaces. The underlying MR image in a–d is the same, and it is a representative slice of a subject brain. (a) Overlay of the brain slice and the cortical surface extracted from the subject brain (red curves). (b) The model's surface warped by a volumetric warping step (green curves). (c) The warped model surface further refined by a surface warping step (blue curves). (d) Overlay of the brain slice and above three surfaces. The orange arrows indicate the positions where the registration results were significantly improved by the surface warping step.

Table 1
Evaluation of registration performance on four real brain images

Subject	M–S distance (mm)		S–M distance (mm)	
	VolWarp	HybWarp	VolWarp	HybWarp
No. 1	0.61	0.31	0.52	0.40
No. 2	0.56	0.37	0.57	0.49
No. 3	0.66	0.45	0.58	0.49
No. 4	0.60	0.37	0.53	0.43

'M' represents a finally warped model surface, and 'S' represents an individual cortical surface. 'M–S' denotes the distance from 'M' to 'S.' 'VolWarp' represents volumetric warping, and 'HybWarp' represents hybrid volumetric and surface warping. The average distance is provided.

registration error of 0.92 mm, and an average maximal registration error of 4.02 mm.

Experiment 2

In this experiment, real brain images are used to visually evaluate the hybrid warping method. Fig. 10 shows the model surface, subject surface, and the warped model surface with and without painted gyri. It can be seen that the subject and the warped model look quite similar, and major gyri of the subject and the warped model are in good correspondence as indicated by the colored curves. To make it easier to visually evaluate those results, we overlay the three surfaces onto the subject volume image in Fig. 11. The areas where the significant registration errors were reduced by the surface warping are indicated by the orange arrows. For those regions where the volumetric warping step has already done a good job, the surface warping changed little. From these visual evaluations, it can be seen that the hybrid warping method has warped the model structures very close to their corresponding counterparts on the subject, and the surface warping has improved the accuracy of volumetric warping.

Experiment 3

Because we do not know the true correspondences among the cortical surfaces in the real data, we used the surface distance to measure the registration accuracy of our algorithm. Although this is not a direct validation method, it does evaluate how well our approach achieves its objective, i.e., to match two surfaces. We note that attribute similarity, and not surface distance, was used as a criterion in the surface warping procedure. Therefore, surface distance is a somewhat independent evaluation criterion. By using the hybrid volumetric and surface warping method, the average distance of finally warped model surfaces to individual surfaces is 0.37 mm, and the average distance of individual surfaces to the finally warped model surfaces is 0.45 mm. Table 1 gives detailed distance measurements of four real brains. It can be seen that the volumetric warping step provided a good initialization, and the surface warping step further refined the warping results. This can be further confirmed by observing a color-coded map of distances of the finally warped model surface to an individual cortical surface in Fig. 12. The average model-to-subject surface distance drops 50% in this case.

Experiment 4

In this experiment, we use the hybrid warping method to automatically label the inner and outer cortical surfaces of a subject. The labels for the inner and outer cortical surfaces of model are obtained by reading the nearest GM labels from a labeled volumetric atlas developed by Dr. Kabani at the Montreal Neurological Institute, including 101 regions of interest. Figs. 13a and 14a show the labels for the inner and outer cortical surfaces of the model. By warping both the inner and outer cortical surfaces of the model along their labels to the subject's inner and outer cortical surfaces, we can label the subject's cortical surfaces, as shown in Figs. 13b and 14b. It can be seen that the automatic labeling results appear visually reasonable. A full-blown validation requires the laborious process of manual painting of sulci and gyri. Such an effort is currently under way in our laboratory in collaboration with other laboratories.

Discussion and conclusion

Topologically correct cortical surface reconstruction is an important step toward cortical structure registration. In addition to methods that perform topology correction to volume images, there are several approaches in the literature that operate directly on the triangulated surface meshes rather than the underlying digital volumes for topology correction. The method reported in Fischl et al. (2001) replaces the manual editing strategy in Dale et al. (1999) by an automatic procedure in which handles are detected as overlapping triangles on the surface after it is inflated to a sphere. The handles are then removed by deleting the overlapping triangles. Another surface-based approach described in Wood (2003) removes small handles by simulating wavefront propagation within a certain neighborhood surrounding each mesh

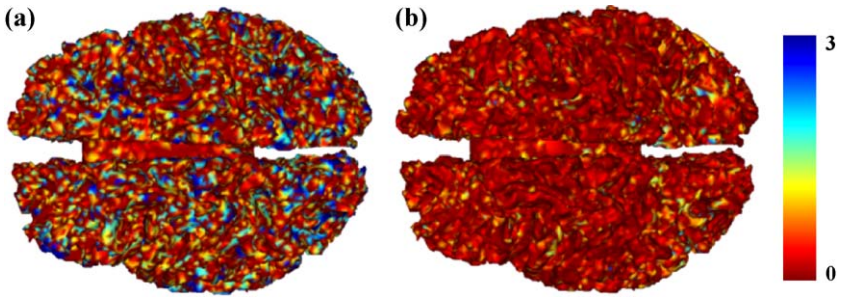

Fig. 12. Color-coded map of surface distances on a real brain. The unit is mm. (a) Surface distances resulting from a volumetric warping step. (b) Surface distances resulting from the hybrid volumetric and surface warping method.

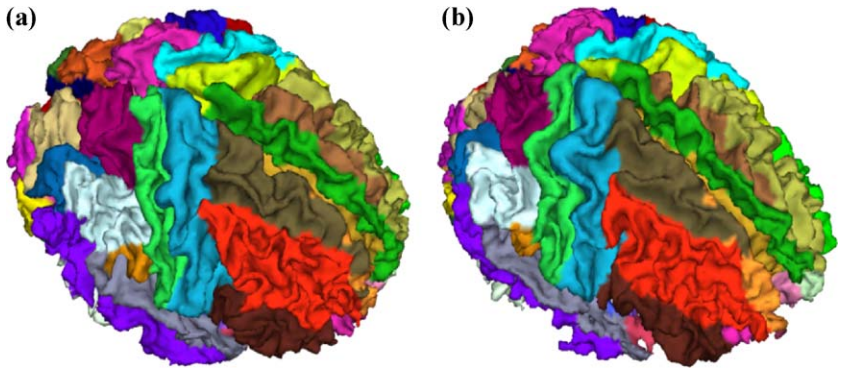

Fig. 13. (a) Model surface, labeled at the Montreal Neurological Institute. (b) Subject surface, labeled after transforming the labels of (a) onto (b) via the proposed surface warping methods.

vertex, after the construction of augmented Reeb graph for the surface. Although many topology correction methods, either based on volume image or surface, are available for the reconstruction of cortical surfaces, none of these methods is optimal in any sense (Han et al., 2002). So, the reconstruction of cortical surface from MR image remains an open research problem.

The remarkable variability in human brain cortex, which brings about the problem of many local minima, has greatly troubled the registration of brain volume images or cortical surfaces. The adaptive deformation method used in this paper is straightforward, and the scheme of defining confidence in cortical structures is limited. Better approaches to studying the variability of brain cortex as well as better strategies to deal with the problem of structure difference in brain image registration across individuals remains an open research issue. Notably, the structural representation approach integrating architectural information of the brain proposed in Mangin et al. (2004) may be a good way to study the variability of the human brain cortex.

In summary, this paper presents a hybrid volumetric and surface warping method for deformable registration of human cortical structures. The volumetric warping based on the HAMMER algorithm considerably removes the variability existing between the cortical surfaces of the model and the individual, and provides a good initialization for the sequent surface-based registration. The volumetric warping in this paper is independent of the surface warping, and is only used to initialize the surface warping. Actually, surface registration result can be used as a feedback to the volumetric warping algorithm, to further improve the accuracy of image registration results. Obviously, the loop of hybrid warping and its feedback to volumetric warping can be repeated until the accuracy of registration stops increasing. Implementing such an approach is one of our future goals. Moreover, we will perform computational optimization to current implementation, which in average requires about 4 h given our computing environments: SGI Origin 300 (600-MHz CPU, 2-Gb memory).

Following the volumetric warping, the clamp histogram of the angles of the normal vectors, which incorporates both local and global geometric information of surfaces, is used to provide a set of attributes that guide the surface warping. To calculate consistent clamp histograms across individuals, we perform topology correction and reconstruct topologically equivalent cortical surfaces. To address the problem of local minima in energy function minimization, we employed the use of a highly distinctive attribute vector and an adaptive deformation strategy. To prevent self-intersection of the model surface during deformation, we used explicit self-intersection prevention in each step of the deformation. Though there are challenges in surface-based methods, we believe that a surface-based method is a promising approach to map the structure or functionality of human brain (Van Essen et al., 1998), or to understand and measure the brain variability (Cachia et al., 2003), as the intrinsic topology of the cerebral cortex is that of a 2-D sheet.

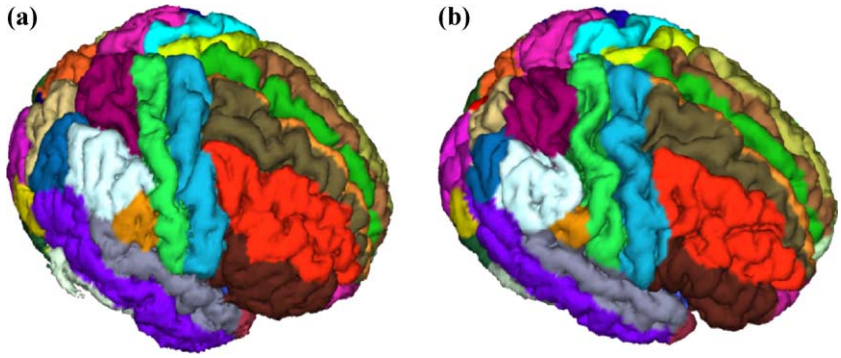

Fig. 14. (a) Model surface, labeled at the Montreal Neurological Institute. (b) Subject surface, labeled after transforming the labels of (a) onto (b) via the proposed surface warping methods.

Acknowledgments

This work was supported by NIH grant R01 AG14971 and by NIH grant R01 NS42645. Images were acquired as part of the neuroimaging study of the Baltimore Longitudinal Study of Aging (BLSA).

References

Abrams, L., Fishkind, D.E., Priebe, C.E., 2002. A proof of the spherical homeomorphism conjecture for surfaces. IEEE Trans. Med. Imag. 21 (12), 1564–1566.

Angenent, S., Haker, S., Tannenbaum, A., Kikinis, R., 1999. On the Laplace–Beltrami operator and brain surface flattening. IEEE Trans. Med. Imag. 18 (8), 700–711.

Ashburner, J., Friston, K.J., 1997. Multimodal image coregistration and partitioning: a unified framework. NeuroImage 6 (3), 209–217.

Ashburner, J., Andersson, J.L.R., Friston, K.J., 1999. High-dimensional image registration using symmetric priors. NeuroImage 9, 619–628.

Ashburner, J., Csernansky, J.G., Davatzikos, C., Fox, N.C., Frisoni, G.B., P.M., P.M., Thompson, P.M., 2003. Computer-assisted imaging to assess brain structure in healthy and diseased brains. Lancet Neurol. 2 (2), 79–88.

Bajcsy, R., Lieberson, R., Reivich, M., 1983. A computerized system for the elastic matching of deformed radiographic images to idealized atlas images. J. Comput. Assist. Tomogr. 7 (4), 618–625.

Bertrand, G., 1994. Simple points, topological numbers and geodesic neighborhoods in cubic grids. Pattern Recogn. Lett. 15, 1003–1011.

Cachia, A., Mangin, J.F., Riviere, D., Kherif, F., Boddaert, N., Andrade, A., Papadopoulous-Orfanos, D., Poline, J.B., Bloch, I., Zilbovicius, M., Sonigo, P., Brunelle, F., Regis, J., 2003. A primal sketch of the cortex mean curvature: a morphogenesis based approach to study the variability of the folding patterns. IEEE Trans. Med. Imag. 22 (6), 754–765.

Christensen, G.E., Rabbit, R.D., Miller, M.I., 1996. Deformable templates using large deformation kinematics. IEEE Trans. Image Process. 5 (10), 1435–1447.

Chui, H., 2001. Non-rigid point matching: algorithms, extensions and applications, PhD dissertation, Yale University.

Collins, D.L., Neelin, P., Peters, T.M., Evans, A.C., 1994. Automatic 3D inter-subject registration of MR volumetric data in standardized Talairach space. J. Comput. Assist. Tomogr. 18 (2), 192–205.

Cormen, T.H., Leiserson, C.L., Rivest, R.L., 1990. Introduction to Algorithms MIT Press, Cambridge, MA.

Crum, W.R., Griffin, L.D., Hill, D.L.G., Hawkes, D.J., 2003. Zen and the art of medical image registration: correspondence, homology, and quality. NeuroImage 20, 1425–1437.

Dale, A.M., Fischl, B., Sereno, M.I., 1999. Cortical surface-based analysis I: segmentation and surface reconstruction. NeuroImage 9, 179–194.

Davatzikos, C., 1997. Spatial transformation and registration of brain images using elastically deformable models. Comput. Vis. Image Underst. 66 (2), 207–222.

Davatzikos, C., Bryan, N., 1996. Using a deformable surface model to obtain a shape representation of the cortex. IEEE Trans. Med. Imag. 15 (6), 785–795.

Davatzikos, C., Bryan, R.N., 2002. Morphometric analysis of cortical sulci using parametric ribbons: a study of the central sulcus. J. Comput. Assist. Tomogr. 26 (2), 298–307.

Dorai, C., Jain, A.K., 1997. COSMOS: a representation scheme for 3d free-form objects. IEEE Trans. Pattern Anal. Mach. Intell. 19 (10), 1115–1130.

Evans, A.C., Dai, W., Collins, L., Neeling, P., Marett, S., 1991. Warping of a computerized 3-D atlas to match brain image volumes for quantitative neuroanatomical and functional analysis. SPIE Proc., Image Process. 1445, 236–246.

Feldmar, J., Ayache, N., 1994. . Locally Affine Registration of Free-Form Surfaces. Computer Vision and Pattern Recognition, Seattle, WA, pp. 496–501.

Fischl, B., Sereno, M.I., Dale, A.M., 1998. Cortical surface-based analysis II: inflation, flattening, a surface-based coordinate system. NeuroImage 9, 195–207.

Fischl, B., Sereno, M.I., Tootell, R., Dale, A.M., 1999. High-resolution intersubject averaging and a coordinate system for the cortical surface. Hum. Brain Mapp. 8, 272–284.

Fischl, B., Liu, A., Dale, A.M., 2001. Automated manifold surgery: constructing geometrically accurate and topologically correct models of the human cerebral cortex. IEEE Trans. Med. Imag. 20, 70–80.

Gee, J.C., Barillot, C., Briquer, L.L., Haynor, D.R., Bajcsy, R., 1994. Matching structural images of the human brain using statistical and geometrical image features. Proc. SPIE Vis. Biomed. Comput. 2359, 191–204.

Goldszal, A.F., Davatzikos, C., Pham, D.L., Yan, M.X.H., Bryan, R.N., Resnick, S.M., 1998. An image processing system for qualitative and quantitative volumetric analysis of brain images. J. Comput. Assist. Tomogr. 22 (5), 827–837.

Han, X., Xu, C., Braga Neto, U., Prince, J.L., 2002. Topology correction in brain cortex segmentation using a multiscale, graph based algorithm. IEEE Trans. Med. Imag. 21 (2), 109–121.

Han, X., Xu, C., Prince, J.L., 2003. A topology preserving level set method for geometric deformable models. IEEE Trans. Pattern Anal. Mach. Intell. 25 (6), 755–768.

Johnson, H.J., Christensen, G.E., 2002. Consistent landmark and intensity-based image registration. IEEE Trans. Med. Imag. 21 (5), 450–461.

Johnson, A.E., Hebert, M., 1999. Using spin-images for efficient multiple model recognition in cluttered 3-D scenes. IEEE Trans. Pattern Anal. Mach. Intell. 21 (5), 433–449.

Joshi, S.C., Miller, M.I., Christensen, G.E., Banerjee, A., Coogan, T., Grenander, U., 1996. Hierarchical brain mapping via a generalized Dirichlet solution for mapping brain manifolds. Proc. SPIE Conf. Geom. Methods Appl. Imag. 2573, 278–289.

Karacali, B., Davatzikos, C., 2003. Topology preservation and regularity in estimated deformation fieldsInformation Processing in Medical Imaging. Ambleside, UK.

Kikinis, R., Jolesz, F.A., Lorensen, W.E., Cline, H.E., Stieg, P.E, Black, P., 1991. 3D reconstruction of skull base tumors from MRI data for neurosurgical planning. Proceedings of the Society of Magnetic Resonance in Medicine Conference.

Kong, T.Y., Rosenfeld, A., 1989. Digital topology: introduction and survey. Comput. Vis. Graph., Image Process. 48, 357–393.

Kriegeskorte, N., Goebel, R., 2001. An efficient algorithm for topologically correct segmentation of the cortical sheet in anatomical MR volumes. NeuroImage 14 (2), 329–346.

Le Goualher, G., Procyk, E., Collins, L., Venegopal, R., Barillot, C., Evans, A., 1999. Automated extraction and variability analysis of sulcal neuroanatomy. IEEE Trans. Med. Imag. 18, 206–216.

Liu, T., Shen, D., Davatzikos, C., 2003. Deformable Registration of Cortical Structures Via Hybrid Volumetric and Surface Warping MICCAI, Montreal, Canada.

Lorensen, W.E., Cline, H.E., 1987. Marching cubes: a high resolution 3D surface construction algorithm. Comput. Graph. 21 (4), 163–169.

MacDonald, D., Kabsni, N., Avis, D., Evans, A.C., 2000. Automated 3-D extraction of inner and outer surfaces of cerebral cortex from MRI. NeuroImage 12, 340–355.

Mangin, J.F., Frouin, V., Bloch, I., Regis, J., Lopez-Krahe, J., 1995. From 3D magnetic resonance images to structural representations of the cortex topography using topology preserving deformations. J. Math. Imaging Vis. 5, 297–318.

Mangin, J.F., Rivière, D., Cachia, A., Papadopoulos-Orfanos, D., Collins, D.L., Evans, A.C., Régis, J., 2003. Object-Based Strategy for Morphometry of the Cerebral Cortex. IPMI, Ambleside, UK.

Mangin, J.F., Rivière, D., Coulon, O., Poupon, C., Cachia, A., Cointepas, Y., Poline, J.B., Le Bihan, D., Régis, J., Papadopoulos-Orfanos, D.,

2004. Coordinate-based versus structural approaches to brain image analysis. Artif. Intell. Med. 30 (2), 177–197.
May, A., Ashburner, J., Büchel, C., McGonigle, D.J., Friston, K.J.R., Frackowiak, S.J., Goadsby, P.J., 1999. Correlation between structural and functional changes in brain in an idiopathic headache syndrome. Nat. Med. 5 (7), 836–838.
McInerney, T., Terzopoulos, D., 1996. Deformable models in medical image analysis: a survey. Med. Image Anal. 1 (2), 91–108.
Möller, T., 1997. A fast triangle–triangle intersection test. J. Graphics Tools 2 (2), 25–30.
Musse, O., Heitz, F., Armspach, J.P., 2001. Topology preserving deformable image matching using constrained hierarchical parametric models. IEEE Trans. Image Process. 10 (7), 1081–1093.
Nielson, G.M., Hamann, B., 1991. The asymptotic decider: resolving the ambiguity in marching cubes. IEEE Vis., 83–91.
Rueckert, D., Sonoda, L.I., Hayes, C., Hill, D., Leach, M.O., Hawkes, D., 1999. Nonrigid registration using free-form deformations: application to breast MR images. IEEE Trans. Med. Imag. 18 (8), 712–721.
Saha, P.K., Chaudhuri, B.B., 1994. Detection of 3D simple points for topology preserving transformations with application to thinning. IEEE Trans. Pattern Anal. Mach. Intell. 16, 1028–1032.
Shattuck, D.W., Leahy, R.M., 2001. Graph based analysis and correction of cortical volume topology. IEEE Trans. Med. Imag. 20 (11), 1167–1177.
Shen, D., Davatzikos, C., 2002. HAMMER: hierarchical attribute matching mechanism for elastic registration. IEEE Trans. Med. Imag. 21 (11), 1421–1439.
Shen, D., Davatzikos, C., 2003. Very high resolution morphometry using mass-preserving deformations and HAMMER elastic registration. NeuroImage 18 (1), 28–41.
Shen, D., Herskovits, E.H., Davatzikos, C., 2001. An adaptive-focus statistical shape model for segmentation and shape modeling of 3D brain structures. IEEE Trans. Med. Imag. 20 (4), 257–270.
Sun, Y., Abidi, M.A., 2001. Surface matching by 3D point's fingerprint. IEEE Int. Conf. Comput. Vision 2, 263–269.
Talairach, J., Tournoux, P., 1988. Co-planar Stereotaxic Atlas of the Human Brain Thieme, New York.
Tao, X., Prince, J.L., Davatzikos, C., 2002. Using a statistical shape model to extract sulcal curves on the outer cortex of the human brain. IEEE Trans. Med. Imag. 21 (5), 513–524.
Terzopoulos, D., Fleischer, K., 1988. Deformable models. Vis. Comput. 4 (6), 306–331.
Thirion, J.P., Monga, O., Benayoun, S., Gueziec, A., Ayache, N., 1992. Automatic registration of 3-D images using surface curvature. SPIE Proc. Math. Methods Med. Imaging 1768, 206–216.
Thompson, P.M., Toga, A.W., 1996. A surface-based technique for warping 3-dimensional images of the brain. IEEE Trans. Med. Imag. 15, 1–16.
Thompson, P.M., Mega, M.S., Woods, R.P., Zoumalan, C.I., Lindshield, C.J., Blanton, R.E., Moussai, J., Holmes, C.J., Cummings, J.L., Toga, A.W., 2001a. Cortical change in Alzheimer's disease detected with a disease-specific population-based brain atlas. Cereb. Cortex 11 (1), 1–16.
Thompson, P.M., Cannon, T.D., Narr, K.L., et al., 2001b. Genetic influences on brain structure. Nat. Neurosci. 4 (12), 1253–1258.
Thompson, P.M., Hayashi, K.M., de Zubicaray, G., Janke, A.L., Rose, S.E., Semple, J., Doddrell, D.M., Cannon, T.D., Toga, A.W., 2002. Detecting dynamic and genetic effects on brain structure using high-dimensional cortical pattern matching. Proc. International Symposium on Biomedical Imaging.
Toga, A.W., Mazziotta, J.C., 2000. Brain Mapping: The Systems. Academic Press, San Diego.
Toga, A.W., Thompson, P.M., 2003. Temporal dynamics of brain anatomy. Annu. Rev. Biomed. Eng. 5, 119–145.
Tosun, D., Rettmann, M.E., Prince, J.L., 2003. Mapping techniques for aligning sulci across multiple brains. MICCAI, 862–869.
Van Essen, H., Drury, A., Joshi, S., Miller, M.I., 1998. Functional and structural mapping of human cerebral cortex: solutions are in the surfaces. Proc. Natl. Acad. Sci. 95 (3), 788–795.
Wang, Y., Peterson, B.S., Staib, L.H., 2003. 3D Brain surface matching based on geodesics and local geometry. Comput. Vis. Image Underst. 89 (2/3), 252–271.
Wells, W.M., Viola, P., Atsumi, H., Nakajima, S., Kikinis, R., 1996. Multimodal volume registration by maximisation of mutual information. Med. Image Anal. 1 (1), 35–51.
Wood, Z.J., 2003. Computational topology algorithms for discrete 2-manifolds. PhD dissertation, California Institute of Technology.
Woods, R.P., Grafton, S.T., Watson, J.D.G., Sicotte, N.L., Mazziotta, J.C., 1998. Automated image registration: II. Intersubject validation of linear and nonlinear models. J. Comput. Assist. Tomogr. 22 (1), 153–165.
Xu, C., Pham, D.L., Rettmann, M.E., Yu, D.N., Prince, J.L., 1999. Reconstruction of the human cerebral cortex from magnetic resonance images. IEEE Trans. Med. Imag. 18 (6), 467–480.
Yamany, S.M., Farag, A.A., 2002. Surfacing signatures: an orientation independent free-form surface representation scheme for the purpose of objects registration and matching. IEEE Trans. Pattern Anal. Mach. Intell. 24 (8), 1105–1120.
Zeng, X., Staib, L.H., Schultz, R.T., Duncan, J.S., 1998. Segmentation and measurement of the cortex from 3D MR images. MICCAI, 519–530.
Zhang, D., Hebert, M., 1999. Harmonic maps and their applications in surface matching. IEEE Conf. Comput. Vis. Pattern, 524–530.